Acta Geochim (2026) 45:155–167
https://doi.org/10.1007/s11631-025-00785-8

ORIGINAL ARTICLE

Pressure dependence of the structures and transport properties of supercritical $NaAlSi_3O_8$–H_2O fluids

Ziteng Long[1] · Yicheng Sun[1]

Received: 15 January 2025 / Revised: 3 April 2025 / Accepted: 6 May 2025 / Published online: 29 May 2025

Abstract Supercritical fluids play a crucial role in material transport within Earth's deep interior. Investigating the pressure-dependent atomic structures and transport properties of such fluids is essential for understanding their petrological, chemical, and geophysical behaviors. In this study, we employed first-principles molecular dynamics simulations to explore the structures, self-diffusion coefficients (D), and viscosities (η) of supercritical $NaAlSi_3O_8$–H_2O fluids under conditions of 2000 K and 3–10 GPa, with water contents of 30 wt% and 50 wt%. Our calculations indicate that at a water content of 30 wt%, Q^2 and Q^3 exhibit a certain degree of positive and negative pressure dependence, respectively, while other Q^n species (n represents the number of bridging oxygens connected to Si/Al) show minimal changes. At a water content of 50 wt%, Q^2 and Q^0 exhibit a certain degree of positive and negative pressure dependence, respectively, while other Q^n species show minimal changes. At both water contents, Si–O–H and molecular water in the system exhibit negative pressure dependence, suggesting that the migration of supercritical fluids from deep to shallow regions is accompanied by the release of water. The self-diffusion coefficients in the supercritical $NaAlSi_3O_8$–H_2O fluid follow the order $D_{Na} \approx D_H > D_O > D_{Al} \approx D_{Si}$, with an overall weak negative pressure dependence. By comparing the viscosities of anhydrous and hydrous silicate melts from previous studies, we found that the addition of water caused a transition from negative to positive pressure dependence of viscosity, corresponding to a structural change from polymerization to depolymerization. Additionally, we calculated the fluid mobility $\Delta\rho/\eta$ of supercritical $NaAlSi_3O_8$–H_2O fluids and found that their mobility is several orders of magnitude higher than that of basalt melt and is also significantly greater than that of carbonate melt. As supercritical fluids ascend from deeper to shallower regions, their mobility is further enhanced, significantly contributing to the transport of elements from subducting slabs to the overlying mantle wedge.

Keywords Supercritical fluids · $NaAlSi_3O_8$–H_2O · First-principles · Speciation · Transport properties

1 Introduction

Silicate melts and aqueous fluids are critical carriers for the transport of material and energy in Earth's interior. They play key roles in crust-mantle cycling, magma formation, element migration, and mineralization processes (Manning 2004). Under high temperature and pressure conditions, silicate melts and aqueous fluids exhibit enhanced mutual solubility. This reduces miscibility gaps and can lead to complete miscibility (Makhluf et al. 2020; Shen and Keppler 1997; Tutolo et al. 2015; Zheng et al. 2016), forming a single-phase supercritical geological fluid, hereafter referred to as "supercritical fluid" (Ni et al. 2017). Supercritical fluids exhibit unique physical and chemical properties, including enhanced solubility for elements (Kessel et al. 2005; Zheng et al. 2011), fluid-like viscosity, melt-like wetting properties, and exceptional element transport capacity (Ni et al. 2017, 2025). These properties make supercritical fluids extraordinarily effective in transporting sulfur, carbon, and other volatiles, as well as high field-strength elements, from

Supplementary Information The online version contains supplementary material available at https://doi.org/10.1007/s11631-025-00785-8.

✉ Yicheng Sun
sunyicheng@hhu.edu.cn

[1] College of Oceanography, Hohai University, Nanjing, China

subducting slabs to the mantle wedge (Ni et al. 2017; Wang et al. 2025). Thus, they serve as essential carriers in deep subduction zones and magmatic-hydrothermal systems. The formation and evolution of supercritical fluids are therefore vital to Earth's deep material cycling, particularly in subduction-related magmatism and mineralization processes (Jin et al. 2023; Manning and Frezzotti 2020; Ni 2020).

Previous studies have determined the second critical endpoints for some supercritical fluids, such as $NaAlSi_3O_8$–H_2O (Makhluf et al. 2020; Shen and Keppler 1997; Stalder et al. 2000), SiO_2–H_2O (Hunt and Manning 2012; Kennedy et al. 1962), $KAlSi_3O_8$–H_2O (Mibe et al. 2008), basalt–H_2O (Mibe et al. 2011) and peridotite–H_2O systems (Kessel et al. 2015; Mibe et al. 2007). Supercritical fluids can form when silicate–H_2O systems are above the second critical endpoint. Therefore, these previous studies have laid an important foundation for understanding the properties of supercritical geofluids. However, research on the physicochemical properties of supercritical fluids remains insufficient. The $NaAlSi_3O_8$–H_2O system is often used as a typical pseudo-binary simple model to understand the fundamental properties of supercritical fluids in subduction zones. Shen and Keppler (1997) used hydrothermal diamond-anvil cell experiments to study the $NaAlSi_3O_8$–H_2O system, directly observing for the first time the process of phase boundary disappearance. Makhluf et al. (2020) used a piston-cylinder apparatus to measure the second critical endpoint (SCEP) of this system as 932 K and 1.63 GPa, respectively. Audétat and Keppler (2004) measured the viscosity of $NaAlSi_3O_8$–H_2O systems (873–1223 K, 1–2 GPa) using the falling sphere method and found that viscosity decreases exponentially with water content up to 20 wt% H_2O. However, as the water content continues to increase, the viscosity of $NaAlSi_3O_8$–H_2O system almost linearly decreases to that of pure water. Sun et al. (2023) explained the relationship between viscosity and microstructures from an atomic perspective, finding that the proportion of high Q^n species rapidly decreases when water is added to silicate melts, replaced by more depolymerized or partially polymerized protonated silicate units, which is the reason for the low viscosity. Fluid inclusions in pegmatites, highly enriched in elements such as Be, B, Cl, P, As, Cs, and certain ore-forming elements (e.g., Sn, Ta), provide indirect evidence of supercritical fluid activity (Thomas and Davidson 2016; Thomas and Rericha 2025; Thomas et al. 2012). Recently, Jin et al. (2023) analyzed multiphase fluid inclusions in ultrahigh-pressure metamorphic veins in subduction zones, discovering that the fluids preserved in these inclusions exhibit supercritical properties and compositional characteristics. In the subduction zones, silicate composition, water content, temperature, and pressure are considered the main factors influencing the structure and transport properties of supercritical $NaAlSi_3O_8$–H_2O fluids. Based on SiO_2 solubility data, Newton and Manning (2002) and Hunt and Manning (2012) conducted thermodynamic modeling, showing that under the SCEP condition (1 GPa, 1353 K), polymerization in SiO_2–H_2O fluids increases with SiO_2 concentration. Previous studies have also highlighted the significant impact of water content on the viscosity of supercritical fluids and preliminarily explored temperature effects (Audétat and Keppler 2004; Sun et al. 2023). However, the pressure dependence of structures and transport properties remains poorly understood. The mobility of supercritical fluids is controlled by their viscosity and density (McKenzie 1989). The migration process of supercritical fluids from deep to shallow regions is accompanied by a decrease in pressure. This pressure reduction may affect the viscosity and density of supercritical fluids. Therefore, investigating the pressure effect is of significant importance for understanding the migration of supercritical fluids. Furthermore, previous research has elucidated the effects of water and temperature on the transport properties and structures of the supercritical $NaAlSi_3O_8$–H_2O system (Sun et al. 2023). Investigating the influence of pressure will provide a more comprehensive understanding of this typical model system and better constrain the factors controlling its transport behavior. This contributes to the evaluation of element migration from subducting slabs to the mantle wedge.

The water content of typical supercritical geofluids ranges from 20 wt% to 80 wt% (Ni et al. 2025). Therefore, to ensure that our research subject is in a supercritical geofluid state, and to understand the pressure effects under different water contents, we selected systems with water contents of 30 wt% and 50 wt% as our research objects. This study uses first-principles molecular dynamics (FPMD) to investigate the structures, species, self-diffusion coefficients, and viscosity of supercritical $NaAlSi_3O_8$–H_2O systems with 30 wt% H_2O and 50 wt% H_2O at 2000 K. We obtained the variation trends of these properties under different pressures and discussed the changes in the coordination of network-forming ions (Si/Al) and the relationship between viscosity and polymerization driven by pressure. The research reveals the pressure dependence of the structures and transport properties of supercritical fluids and explores the impact of pressure on the behavior of supercritical fluids in subduction zones. The temperature employed in this study are higher than those found in actual subduction zones. This is due to the significant challenges (convergence difficulties) associated with obtaining the transport properties of the system using first-principles methods at lower temperatures. Nevertheless, this study provides qualitative insights, and the qualitative understanding of pressure effects obtained herein remains applicable at lower temperatures.

2 Computational methods

First principles molecular dynamics (FPMD) simulations of $NaAlSi_3O_8$–H_2O systems were performed in the DFT code VASP (Kresse and Hafner 1993, 1994; Kresse and Furthmüller 1996a, b). The Perdew-Burke-Ernzerhof (PBE) functional (Perdew et al. 1996) was used with Grimme–D3 dispersion correction (Grimme et al. 2010). A plane wave cut-off of 520 eV and gamma point Brillouin zone sampling were used. The convergence of k-point mesh and cutoff energy were tested and found to converge the total energy to within 1 meV/atom and 2 meV/atom, respectively. Our simulations were performed in the NVT ensemble with a time step of 0.5 fs. To understand the effect of pressure on supercritical fluids at different water contents, we conducted studies on systems with 30 wt% (254 atoms) and 50 wt% (232 atoms) water content in the pressure range of 3 GPa to ~10 GPa. These two water contents represent relatively low and high water contents in the supercritical $NaAlSi_3O_8$–H_2O fluids, respectively. The initial equilibrium structures at 2000 K are from a previous study (Sun et al. 2023). For each model, we first calculated the pressure of the models under different volumes to obtain the pressure–volume curves. Then, the volume corresponding to approximately 3–10 GPa (Table 1) was obtained and simulated for at least 60 ps. The temperature and pressure ranges calculated in our study are all above the critical curve of supercritical $NaAlSi_3O_8$–H_2O fluids (Supplementary Fig. S1).

To validate the size effect of this system, we employed classical molecular dynamics simulation. We constructed two systems of different sizes with the same density and a water content of 50 wt%. The large system contains 1856 atoms, and the small system contains 232 atoms, where the small system model is exactly the same as the model used in the first-principles method in this study. The details of the simulation can be found in the supplementary material (Text S1). The results of the classical molecular dynamics simulation show that the results for H, O, and Q^n species are very close between the 232-atom model and the 1856-atom model (Supplementary Fig. S10). This indicates that the system size used in this study can already obtain reasonable results.

Self-diffusion coefficients were calculated using the Einstein relation (Allen et al. 1989). Shear viscosity was derived from the stress autocorrelation function (ACF) via the Green–Kubo relation (Allen et al. 1989). Three off-diagonal components of the stress tensor were employed to compute the shear viscosity. Pairwise radial distribution functions (RDFs) were used to analyze structural properties (Supplementary Fig. S2).

Table 1 Calculated pressure of the $NaAlSi_3O_8$–H_2O system at 2000 K

H_2O (wt%)	Number of atoms	Density (g cm^{-3})	Pressure (GPa)
30.04	254	1.91	3.53 ± 0.07
30.04	254	2.05	4.97 ± 0.07
30.04	254	2.20	7.08 ± 0.07
30.04	254	2.38	10.22 ± 0.08
50.75	232	1.67	4.52 ± 0.05
50.75	232	1.79	6.08 ± 0.06
50.75	232	1.93	8.16 ± 0.06
50.75	232	2.03	10.20 ± 0.06

3 Results

3.1 Q^n species

In the silicate-water system, we use Q^n to describe the network structure of silicate fluids, where n represents the number of bridging oxygens (BO) connected to Si/Al. Pressure can break bridging oxygen (BO) bonds (Si/Al–O–Si/Al), leading to changes in the distribution of Q^n species (Wang et al. 2014). For example, in hydrous $NaAlSi_2O_6$ (~4 wt% H_2O) melts, the coordination number of Si/Al can increase to 5 or even 6 under high pressure (Bajgain et al. 2019). In such cases, the proportion of Q^4 species decreases, while Q^5 and Q^6 species increase. However, the pressure dependence of Q^n species in supercritical $NaAlSi_3O_8$–H_2O fluids is not obvious. As shown in Fig. 1, we calculated the Q^n species of supercritical $NaAlSi_3O_8$–H_2O systems with 30 wt% and 50 wt% H_2O at different pressures at 2000 K. The results indicate that in the 30 wt% H_2O system, the proportions of Q^2 and Q^3 species are the highest, while those of Q^0 and Q^5 species are the lowest. With increasing pressure, the proportion of Q^2 species gradually increases, while that of Q^3 species generally decreases. We infer that Q^3 species convert to Q^2 species with increasing pressure (mainly in the range of 3.53 to 7.08 GPa). The proportions of Q^1 and Q^4 species show a slight decreasing trend with increasing pressure. The proportion of Q^0 species shows minimal variation with pressure, remaining relatively stable across the studied pressure range. The proportion of Q^5 species slightly increases with pressure. Additionally, the trend in the average n of Q^n is not significantly affected by pressure. In the 50 wt% H_2O system, the proportions of Q^1 and Q^2 species are the highest, while those of Q^4 and Q^5 species are the lowest. Under pressure, the proportion of Q^2 species increases slowly (from an initial 32% to a maximum of 41% at 10.20 GPa). The proportion of Q^0 species shows a continuous decreasing trend (from an initial 17% to a minimum of 5% at 10.20 GPa). The proportions of Q^1, Q^3, Q^4, and Q^5 species show slight changes with increasing pressure. Compared with the 30

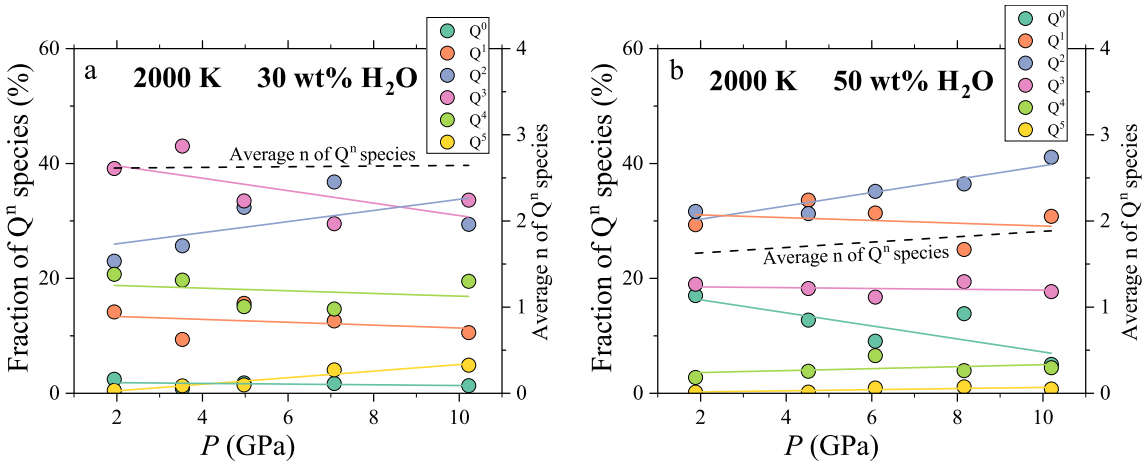

Fig. 1 Relationship between Q^n species and pressure in supercritical $NaAlSi_3O_8$–H_2O systems with **a** 30 wt% H_2O and **b** 50 wt% H_2O. The black dashed lines represent the average value of n in Q^n, corresponding to the right y-axis. Data for 30 wt% H_2O at 1.94 GPa and 50 wt% H_2O at 1.88 GPa are from Sun et al. (2023). The solid lines represent linear fits to the data, serving to facilitate an overall understanding of the data trends

wt% H_2O system, the average value of Q^n in the 50 wt% H_2O system shows a continuous increasing trend with pressure.

The occurrence of Q^5 is correlated with changes in the coordination number within the system. With increasing pressure, both 4-coordinated Si and Al decrease, corresponding to an increase in 5-coordinated Si and 5- and 6-coordinated Al (Supplementary Fig. S6a and b). The average coordination number of Si shows little variation within the considered pressure range, while the average coordination number of Al exhibits a slight increase (Supplementary Fig. S6d and f).

In summary, increasing pressure results in an increase in the proportion of Q^2 species in both systems, accompanied by a decrease in Q^3 species in the 30 wt% H_2O system and a decrease in Q^0 species in the 50 wt% H_2O system. Additionally, increasing the water content from 30 wt% to 50 wt% causes depolymerization of the fluid structure, with the effect of water being greater than that of pressure.

3.2 H and O species and polymerization degree

In the supercritical $NaAlSi_3O_8$–H_2O system, hydrogen mainly exists in the forms of H_2O and Si/Al–O–H (with one hydrogen atom bonded to a non-bridging oxygen, labeled as NBO–H) (Fig. 2a). Oxygen primarily exists as bridging oxygen (BO, an oxygen atom connected to multiple network formers), non-bridging oxygen (NBO, an oxygen atom connected to only one network former), free oxygen (FO, oxygen in a free state), molecular water (H_2O_m), free hydroxyl (OH), and H_3O (an oxygen atom connected to three hydrogen atoms). Overall, the proportions of H_2O and NBO–H in both systems decrease with increasing pressure. Correspondingly, the proportions of BO–H (one hydrogen atom bonded to a bridging oxygen) and NBO–H_2 (two hydrogen atoms bonded to a non-bridging oxygen) increase (Fig. S8). Additionally, we conducted a detailed analysis of the oxygen species in both systems. The differences in oxygen species distribution between the two systems are mainly due to the reaction of water with BO (Sun et al. 2023). Increasing water content disrupts the aluminosilicate network and drives depolymerization (Mysen 2014). In the 30 wt% H_2O system, NBO content is the highest (36%–45%), followed by BO (34%–39%), with the lowest content found in other oxygen species (FO, OH, H_3O, and H_2O_m). With increasing pressure, the proportion of other oxygen species decreases (Fig. 2d), reaching a minimum of 18% at 10.22 GPa. The proportion of BO remains relatively stable, showing a weak dependence on pressure (Fig. 2b), while the proportion of NBO shows a slight increase with increasing pressure (Fig. 2c). The NBO/T (T = Si, Al) value in the 30 wt% H_2O system shows a slight increasing trend with pressure (Fig. 2e). In the 50 wt% H_2O system, the other oxygen species have the highest content (41%–44%), followed closely by NBO (40%–42%), with BO having the lowest content (13%–16%). With increasing pressure, the contents of NBO, BO, and other oxygen species show minimal changes. The NBO/T value in the 50 wt% H_2O system is less affected by pressure, remaining around 2.4. In summary, compared to the 30 wt% H_2O system, the H (mainly H_2O and NBO–H) and O species in the 50 wt% H_2O system are less sensitive to pressure. The increasing water content may weaken the pressure effect on the proportions of H and O species.

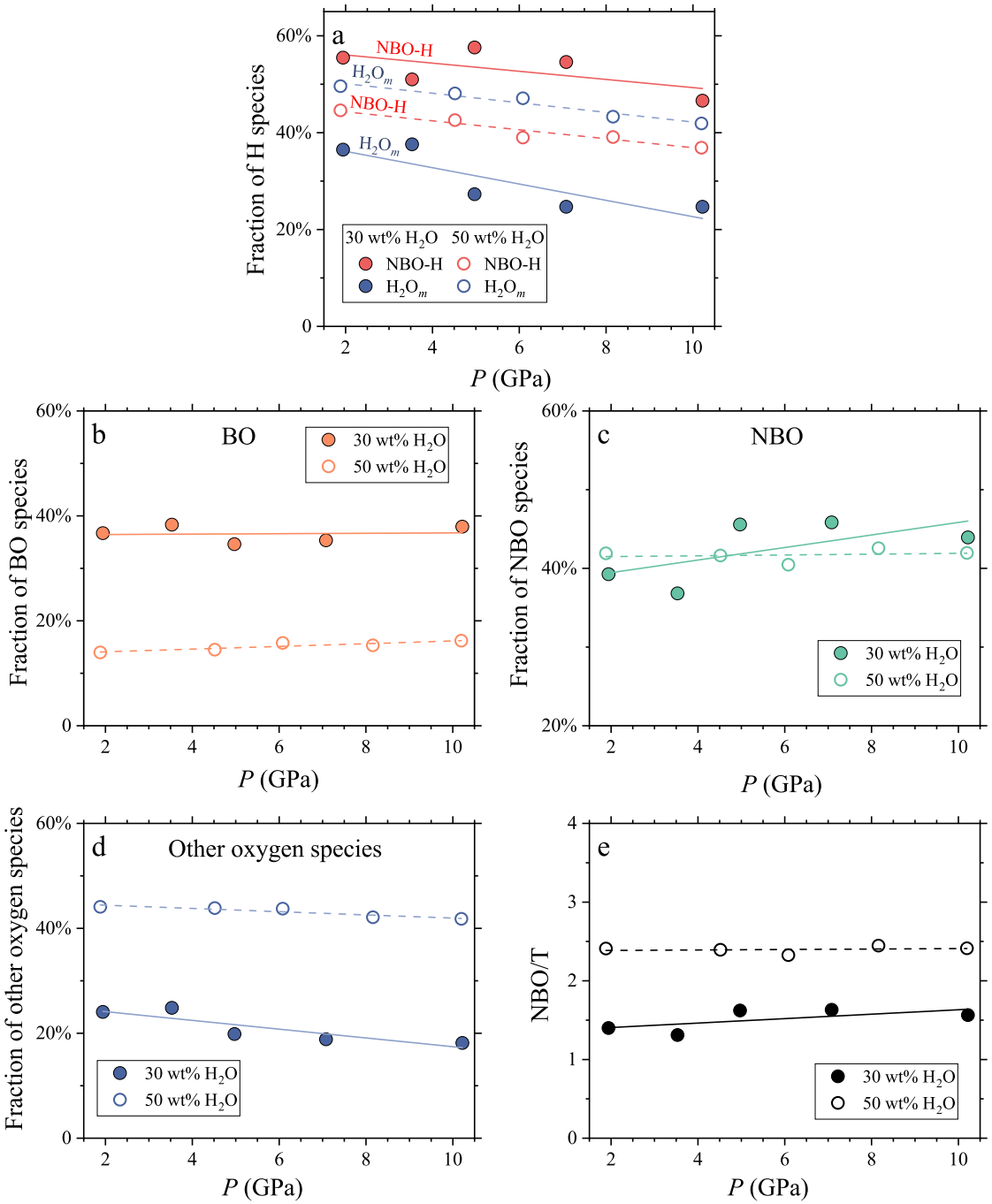

Fig. 2 Pressure dependent behavior of **a** hydrogen species, **b–d** oxygen species and **e** NBO/T in the $NaAlSi_3O_8$–H_2O systems at 30 wt% and 50 wt% H_2O. The solid lines represent linear fits to the data, serving to facilitate an overall understanding of the data trends

3.3 Self-diffusion

The self-diffusion coefficients of various elements in $NaAlSi_3O_8$–H_2O systems with water contents of 30 wt% and 50 wt% at 2000 K under different pressures are shown in Fig. 3 (the corresponding mean square displacement can be found in Supplementary Figs. S3 and S4). The order of self-diffusion coefficients is $D_{Na} \approx D_H > D_O > D_{Al} \approx D_{Si}$, which is similar to the diffusion sequence of elements in hydrous $NaAlSi_2O_6$ (4.2 wt% H_2O) melt at 2500 K reported by Bajgain et al. (2019). Within the studied pressure range, the self-diffusion coefficients of Na, O, and H decrease with increasing pressure, and the D_{Na} and D_H are significantly higher than those of network-forming ions (Si/Al), particularly around 2 GPa. In the 30 wt% H_2O system, D_{Na} is about 15 times that of D_{Si} or D_{Al}, and D_H is about 10 times that of

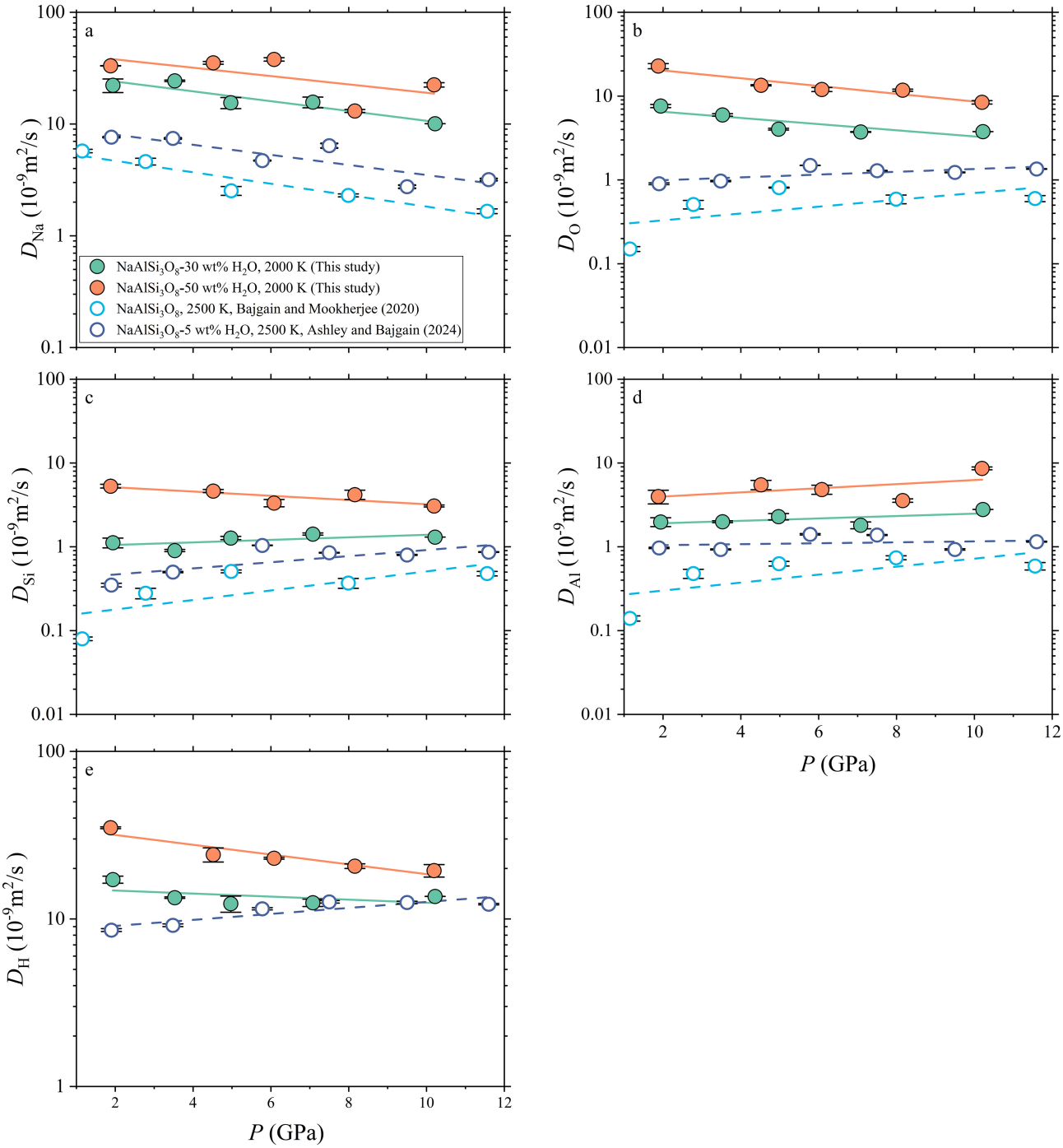

Fig. 3 **a–e** Comparison of self-diffusion coefficients at 2000 K in supercritical $NaAlSi_3O_8$–H_2O systems with 30 wt% H_2O and 50 wt% H_2O with FPMD results at 2500 K for $NaAlSi_3O_8$ melt (Bajgain and Mookherjee 2020) and hydrous (5 wt% H_2O) $NaAlSi_3O_8$ melt (Ashley et al. 2024). The error bar of the self-diffusion coefficient was obtained using the standard error from the fitted mean squared displacement. The solid lines represent linear fits to the data, serving to facilitate an overall understanding of the data trends

D_{Si} or D_{Al}. In the 50 wt% H_2O system, D_{Na} is about 6 times that of D_{Si} or D_{Al}, and D_H is about 5 times that of D_{Si} or D_{Al}. This difference is mainly because Na atom, with its larger atomic radius and lower field strength compared to Si or Al, have diffusion rates primarily dependent on valence and radius size, exhibiting lower activation energies and negative pressure dependence (referred to as intrinsic diffusivity) (Dingwell 2006). Additionally, the weak bonding of Na with O ions allows Na to easily dissociate and move. Thus, Na can traverse the fluid structure more freely, diffusing rapidly

at lower pressure. However, as pressure increases and free space progressively collapses, the self-diffusion rate of Na decreases. H mainly exists as NBO–H (Si–O–H) and H_2O_m (Fig. 2a), and the presence of a large amount of H_2O_m keeps D_H at a relatively high level. D_O exhibits a trend similar to D_H, showing weak negative pressure dependence, as most H and O diffuse together in the forms of NBO–H and H_2O_m. As network-forming cations, Si has a lower self-diffusion rate. In the 30 wt% H_2O system, D_{Si} shows a weak positive correlation with pressure. In the 50 wt% H_2O system, D_{Si} gradually decreases with increasing pressure, consistent with the trend observed in depolymerized $CaMgSi_2O_6$ melts (Reid et al. 2001). At a constant pressure, D_{Al} is slightly higher than D_{Si}, and D_{Al} generally shows a slight increase with increasing pressure. The impact of pressure on ion diffusion usually follows the Arrhenius relationship (Allen et al. 1989):

$$D = D_0 \exp\left(-\frac{E_a + PV_a}{RT}\right) \quad (1)$$

where D_0 is the pre-exponential factor, E_a is the activation energy, V_a is the activation volume, R is the ideal gas constant, and T is the temperature. The key to the positive or negative pressure dependence of the self-diffusion coefficients of elements lies in the sign change of the activation volume. In the 30 wt% H_2O system, the activation volume of D_{Si} is negative, while it is positive in the 50 wt% H_2O system. In both systems, the activation volume of D_{Al} is negative, while those of D_{Na}, D_O, and D_H are positive. A negative activation volume indicates that the activated complex for diffusion is more densely packed than the ground state (Lesher 2010).

In order to determine the impact of water content on self-diffusion rates, we compared the ionic diffusivity in systems with 30 wt% H_2O and 50 wt% H_2O in this study (Table 2). The results indicate that increasing water content decreases the activation energy of the $NaAlSi_3O_8$–H_2O system, consistent with observations for hydrous aluminosilicate melts reported by Ashley et al. (2024). Consequently, the diffusion rates of each element in the 50 wt% H_2O system are significantly higher than those in the 30 wt% H_2O system. This also aligns with the fact that water enhances melt fluidity by disrupting the melt structure (Mysen 2014; Sun et al. 2023).

3.4 Viscosity

Viscosity (η) plays a fundamental role in controlling the flow of silicate melts (Giordano et al. 2008). Early studies on melt viscosity indicated that at low pressures, the effect of pressure is most pronounced on highly polymerized melts, while the impact on depolymerized fluids is minimal or even negligible (Ardia et al. 2008; Fortier and Giletti 1989; Hui et al. 2009; Kushiro 1978). Our FPMD results show that the viscosity of the supercritical $NaAlSi_3O_8$–H_2O fluid with different water contents exhibits a weak positive pressure dependence within the studied pressure range. By comparing the viscosity of the supercritical $NaAlSi_3O_8$–H_2O fluid with anhydrous $NaAlSi_3O_8$ melt (Bajgain and Mookherjee 2020; Mori et al. 2000) and hydrous $NaAlSi_3O_8$ (5 wt% H_2O) melt (Ashley et al. 2024), we found that the pressure dependence of viscosity in supercritical fluids is different from that in polymerized silicate melts. At 2500 K, the viscosity of anhydrous $NaAlSi_3O_8$ melts decreased tenfold when the pressure increased from 1.15 GPa to 11.56 GPa (Fig. 4). The addition of water causes significant depolymerization and viscosity reduction in the melts, greatly weakening this effect. For example, in hydrous $NaAlSi_3O_8$ melts (5 wt% H_2O) at the same temperature, the viscosity remains generally unchanged with increasing pressure (Fig. 4). For $NaAlSi_3O_8$–H_2O fluids at 2000 K, as the water content increases to 30 wt% and 50 wt%, the pressure dependence of viscosity gradually shifts from negative to positive.

4 Discussion

4.1 Pressure dependence of the structure of the supercritical $NaAlSi_3O_8$–H_2O fluids

The structure of silicate fluids is closely related to temperature, pressure, and water content, which significantly influence their physicochemical properties (Audétat and Keppler 2004; Mysen 2014). In supercritical $NaAlSi_3O_8$–H_2O fluids, with increasing water content, Q^4 species gradually decrease until they disappear completely, corresponding to a continuous increase in Q^0 species. This occurs because increasing water content promotes the depolymerization of silicates, leading to a transition from higher Q^n species to lower Q^n species (Sun et al. 2023). Previous studies on silicate fluids in subduction zones have shown that increasing pressure increases the solubility of silicates in water, thereby increasing their degree of polymerization (Makhluf et al. 2020; Manning 2004; Newton and Manning 2008). Bajgain et al. (2019) studied the pressure dependence of the structure of anhydrous and hydrous (~4 wt% H_2O) $NaAlSi_2O_6$ melts at 2500 K, finding that within the range of 2–10 GPa, the melt structure adapts to compaction by adjusting bond lengths and coordination numbers, favoring the formation of high coordination numbers for Si–O and Al–O. To understand the pressure dependence of the structure of supercritical $NaAlSi_3O_8$–H_2O fluid, we calculated the coordination environment of different cations. At 2000 K, with increasing pressure, the coordination numbers of Si/Al (especially Al) show more high-coordination species at the expense of low-coordination species, with a decrease in four-coordinated

Table 2 Pre-exponential factors (D_0), activation energies (E_a), and activation volumes (V_a) for the $NaAlSi_3O_8$–H_2O systems with 30 wt% H_2O and 50 wt% H_2O obtained from Arrhenius equation fits (Eq. 1)

Species	Composition	D_0 ($\times 10^{-9}$ $m^2 \cdot s^{-1}$)	E_a ($KJ \cdot mol^{-1}$)	V_a ($cm^3 \cdot mol^{-1}$)
Na	$NaAlSi_3O_8$ (30 wt% H_2O)	1595 ± 94	67 ± 10	1.6 ± 0.4
	$NaAlSi_3O_8$ (50 wt% H_2O)	1919 ± 238	63 ± 2	1.1 ± 0.4
	$NaAlSi_3O_8$ (5 wt% H_2O)[a]	200 ± 100	60 ± 10	5.0 ± 3.0
	$NaAlSi_3O_8$[b]	314 ± 10	72 ± 1	3.2 ± 0.0
	$NaAlSi_2O_6$ (~4 wt% H_2O)[c]	356 ± 66	72 ± 5	2.1 ± 0.1
	$NaAlSi_2O_6$[c]	309 ± 32	77 ± 3	2.0 ± 0.1
Al	$NaAlSi_3O_8$ (30 wt% H_2O)	308 ± 19	86 ± 10	− 0.5 ± 0.2
	$NaAlSi_3O_8$ (50 wt% H_2O)	463 ± 59	83 ± 2	− 1.3 ± 0.3
	$NaAlSi_3O_8$ (5 wt% H_2O)[a]	1100 ± 500	150 ± 10	− 2.0 ± 3.0
	$NaAlSi_3O_8$[b]	1686 ± 190	190 ± 4	− 3.5 ± 0.1
	$NaAlSi_2O_6$ (~4 wt% H_2O)[c]	356 ± 210	129 ± 13	− 2.2 ± 0.5
	$NaAlSi_2O_6$[c]	245 ± 128	136 ± 12	− 2.3 ± 0.4
Si	$NaAlSi_3O_8$ (30 wt% H_2O)	238 ± 14	91 ± 1	− 0.6 ± 0.2
	$NaAlSi_3O_8$ (50 wt% H_2O)	238 ± 13	62 ± 9	1.0 ± 0.1
	$NaAlSi_3O_8$ (5 wt% H_2O)[a]	3000 ± 1000	197 ± 8	− 5.0 ± 3.0
	$NaAlSi_3O_8$[b]	1814 ± 574	199 ± 8	− 3.1 ± 0.2
	$NaAlSi_2O_6$ (~4 wt% H_2O)[c]	255 ± 164	133 ± 14	− 2.0 ± 0.5
	$NaAlSi_2O_6$[c]	221 ± 125	143 ± 13	− 2.5 ± 0.4
O	$NaAlSi_3O_8$ (30 wt% H_2O)	813 ± 60	76 ± 1	1.7 ± 0.2
	$NaAlSi_3O_8$ (50 wt% H_2O)	1595 ± 84	69 ± 1	1.9 ± 0.1
	$NaAlSi_3O_8$ (5 wt% H_2O)[a]	1600 ± 500	165 ± 7	− 3.0 ± 3.0
	$NaAlSi_3O_8$[b]	1535 ± 154	187 ± 2	− 4.1 ± 0.1
	$NaAlSi_2O_6$ (~4 wt% H_2O)[c]	384 ± 248	130 ± 14	− 1.9 ± 0.5
	$NaAlSi_2O_6$[c]	370 ± 179	144 ± 11	− 2.7 ± 0.4
H	$NaAlSi_3O_8$ (30 wt% H_2O)	1151 ± 60	72 ± 1	0.4 ± 0.1
	$NaAlSi_3O_8$ (50 wt% H_2O)	1800 ± 66	65 ± 1	1.2 ± 0.1
	$NaAlSi_3O_8$ (5 wt% H_2O)[a]	1600 ± 400	112 ± 6	− 2.0 ± 2.0
	$NaAlSi_2O_6$ (~4 wt% H_2O)[c]	450 ± 285	83 ± 14	− 0.7 ± 0.4

[a]Hydrous $NaAlSi_3O_8$ melt (5 wt% H_2O) at 2500 K and 0 GPa from Ashley et al. (2024)

[b]Anhydrous $NaAlSi_3O_8$ melt at lower pressures along the 2500 K and 3000 K isotherms from Bajgain and Mookherjee (2020)

[c]Anhydrous and hydrous (~4 wt% H_2O) $NaAlSi_2O_6$ melts at low-pressure regime (~0 – 12 GPa) along the 2500 K and 3000 K isotherms from Bajgain et al. (2019)

Si/Al and an increase in five- and six-coordinated species (Supplementary Fig. S6).

Compared to the continuous shift to higher Q^n species (with a decrease in Q^3 and Q^4 and an increase in Q^5 and Q^6) in hydrous and anhydrous $NaAlSi_2O_6$ melts with increasing pressure (Fig. S9b), the Q^n species in supercritical $NaAlSi_3O_8$–H_2O fluids show weak changes with pressure (Fig. S9a). Additionally, compared to polymerized anhydrous or hydrous silicate melts, the proportion of bridging oxygens (BO) in supercritical $NaAlSi_3O_8$–H_2O fluids is lower, while the proportion of non-bridging oxygens (NBO) is higher (Fig. S9c and d). This is mainly due to the large amount of water in the supercritical fluid, which disrupts the cation-polymerized chains forming the network and creates abundant protonated silicate units (Sun et al. 2023). These bonds are much weaker than T–O bonds, offering a "buffering" mechanism similar to depolymerized fluids for the compression of TO_4 tetrahedra (Wang et al. 2014). This also implies that due to the depolymerizing effect of water, the structure of supercritical fluids resembles that of depolymerized melts when subjected to pressure.

4.2 Pressure dependence of transport properties

Self-diffusion coefficients are unique among transport properties because they refer to specific elements or components rather than the entire system (Ni et al. 2015). We compared the self-diffusion coefficients of elements in supercritical $NaAlSi_3O_8$–H_2O fluids at 2000 K with anhydrous $NaAlSi_3O_8$ melt (Bajgain and Mookherjee 2020) and hydrous (5-wt% H_2O) $NaAlSi_3O_8$ melt (Ashley et al. 2024) at 2500 K (Fig. 3). The results show that dissolved H_2O

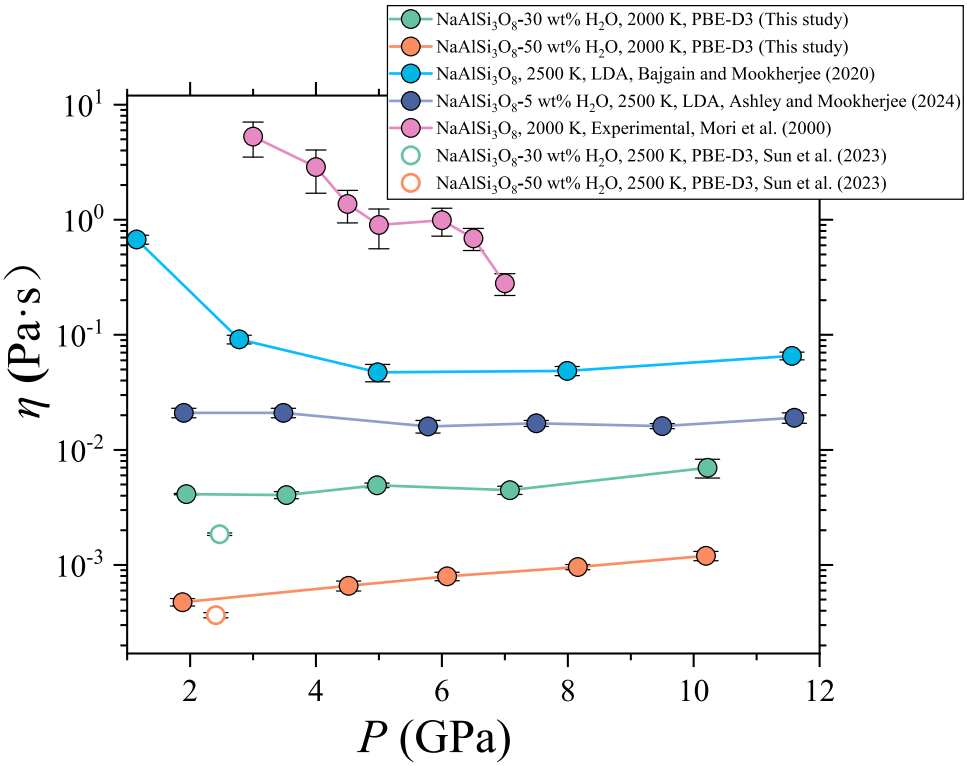

Fig. 4 Variation of viscosity with pressure in $NaAlSi_3O_8$–H_2O systems with 30 wt% and 50 wt% H_2O at 2000 K, compared to $NaAlSi_3O_8$ melts and 5 wt% H_2O $NaAlSi_3O_8$ melts. The data for $NaAlSi_3O_8$ melts at 2000 K and 2500 K are from Mori et al. (2000) and Ashley et al. (2024); Bajgain and Mookherjee (2020). Green and orange open symbols represent the viscosity of systems with 30 wt% H_2O (2.47 GPa) and 50 wt% H_2O (2.41 GPa) at 2500 K, respectively, based on data from Sun et al. (2023). The corresponding stress ACF can be found in Supplementary Fig. S5. The error bar of the viscosity adopted the mean absolute error

affects the pressure dependence of ionic self-diffusion rates by depolymerizing the melt structure at all studied temperatures and pressures. Notably, the pressure dependence of D_H and D_O is negative in supercritical $NaAlSi_3O_8$–H_2O fluids, whereas it is positive in anhydrous or hydrous $NaAlSi_3O_8$ melts. In $NaAlSi_3O_8$ melt with low water content, H transfer mainly occurs between NBO and NBO–H (Karki and Stixrude 2010b; Sun et al. 2023), relying more on NBO self-diffusion, showing positive pressure dependence. In the supercritical $NaAlSi_3O_8$–H_2O fluids, H primarily exists as NBO–H and molecular H_2O_m, with a significant portion of H diffusion controlled by H_2O diffusion. We infer that the negative pressure dependence of D_H may be related to the decreasing proportion of H_2O_m and NBO-H species with increasing pressure (Fig. 2a). In anhydrous and hydrous $NaAlSi_3O_8$ melts, oxygen mainly exists as BO and NBO. Therefore, its self-diffusion behavior is closer to that of Si/Al. In supercritical $NaAlSi_3O_8$–H_2O fluids, oxygen, in addition to forming BO and NBO by bonding with Si/Al, also exists in other oxygen species such as FO, OH, H_3O, and H_2O_m. With increasing pressure, the other oxygen species transform into NBO/BO, and since their self-diffusion rates are higher than those of NBO/BO, the O self-diffusion coefficient decreases with increasing pressure. Within the studied pressure range, the self-diffusion of Si/Al in anhydrous $NaAlSi_3O_8$ melts and hydrous $NaAlSi_3O_8$ melts shows a slight increase with increasing pressure (Fig. 3c and d). In the supercritical $NaAlSi_3O_8$–H_2O systems, the D_{Si} exhibits a relatively weak variation within the error range at 30 wt% H_2O, but shows a significant negative pressure dependence at 50-wt% H_2O. Generally, an increase in pressure leads to a decrease in free volume, thereby reducing the self-diffusivity of elements. Therefore, the decrease in D_{Si} with decreasing pressure at 50-wt% H_2O might be attributed to the reduction of free volume. However, D_{Al} shows a positive pressure dependence at both 30-wt% and 50-wt% H_2O. This may be due to the higher content of 5-coordinated Al (Supplementary Fig. S6b), which act as a transition state for viscous flow in silicates (Karki and Stixrude 2010a), facilitating the self-diffusion of Al.

The pressure dependence of melt viscosity is primarily controlled by structural changes under compression. At low pressures (< 1 GPa), the effect of pressure on the viscosity of hydrous melts is negligible or only slightly dependent on pressure (Ardia et al. 2008; Liebske et al. 2003). At higher pressures, the pressure dependence of hydrous melt viscosity varies depending on the composition and degree of polymerization. Generally, the pressure dependence of melt viscosity is mainly determined by the degree of polymerization (decreasing with increasing NBO/T) (Behrens and Schulze 2003). Within the studied pressure range, the viscosity of highly polymerized melts (NBO/T < 1) usually decreases with increasing pressure. As shown in Fig. 5, the viscosity of anhydrous $NaAlSi_3O_8$ melts (NBO/T ≈ 0) at 2500 K decreases tenfold with increasing pressure (Bajgain and Mookherjee 2020). For

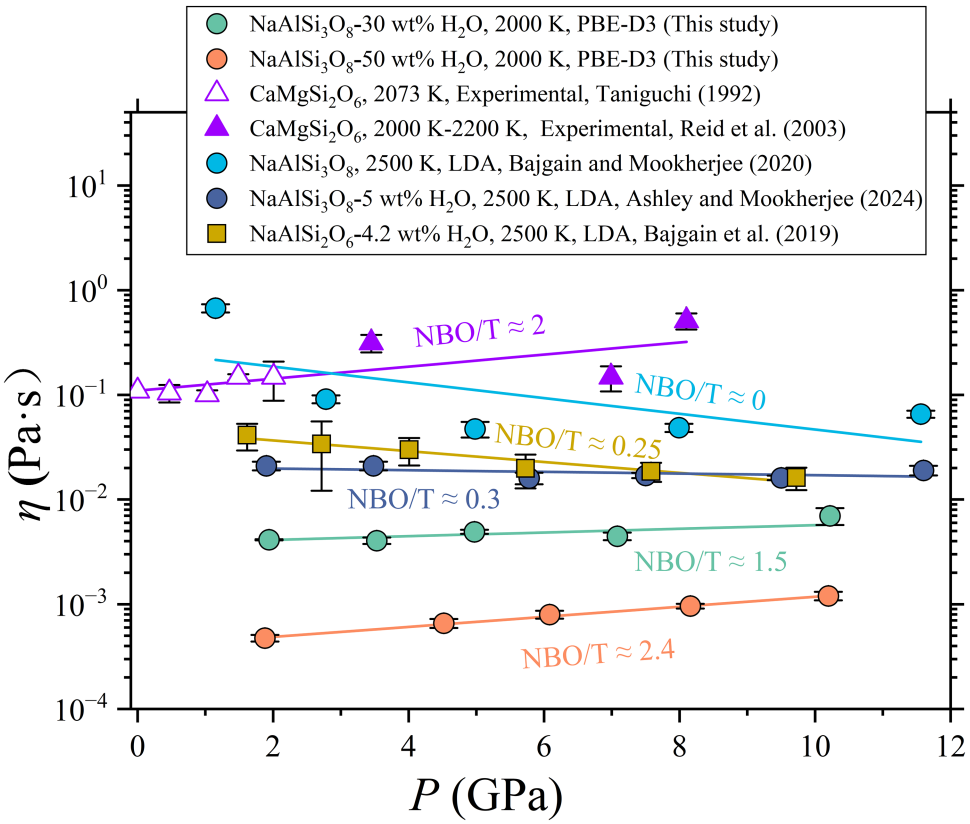

Fig. 5 Comparison of pressure dependence of viscosity between supercritical fluids and anhydrous/hydrous silicate melts. The data for $NaAlSi_3O_8$ melt, hydrous (5-wt% H_2O) $NaAlSi_3O_8$ melt, and hydrous (4.2 wt% H_2O) $NaAlSi_2O_6$ melt are sourced from Bajgain and Mookherjee (2020), Ashley et al. (2024), and Bajgain et al. (2019), respectively. Data for $CaMgSi_2O_6$ melts are sourced from Taniguchi (1992) and Reid et al. (2003)

$NaAlSi_2O_6$ melts with low water content (~4.2-wt% H_2O, NBO/T ≈ 0.25) (Bajgain et al. 2019) and $NaAlSi_3O_8$ melts with ~5-wt% H_2O (NBO/T ≈ 0.3) (Ashley et al. 2024), increasing water content causes melt depolymerization. This leads to a decrease in BO and an increase in NBO, resulting in an increase in NBO/T value. Thus, their viscosity just shows a slight decreasing trend. Conversely, the viscosity of less polymerized melts typically shows a positive pressure dependence (Wang et al. 2014). For instance, at 2000 K, the viscosity of depolymerized $CaMgSi_2O_6$ melts (NBO/T ≈ 2) increases with increasing pressure (Reid et al. 2003; Taniguchi 1992). In this study, the viscosity of the supercritical $NaAlSi_3O_8$–H_2O increases slowly with increasing pressure. Due to the high water content, the system is essentially in a depolymerized state, so the pressure effect on the system's viscosity is similar to the pressure effect on depolymerized silicate melts. Wang et al. (2014) demonstrated that as pressure increases, the coordination number of Si/Al in depolymerized silicate melts increases, leading to further packing of the silicates and an increase in density and viscosity. It can be observed in our study that with the increase of pressure, the Si/Al coordination number increases (Supplementary Fig. S6), thereby allowing further packing of the system, and simultaneously leading to an increase in the viscosity and density.

5 Implications

The high migration ability of supercritical fluids is closely related to their low viscosity (Ni et al. 2017). Following Darcy's law (McKenzie 1989), gravity-driven fluid transportation is proportional to fluid mobility, $\Delta\rho/\eta$, where $\Delta\rho$ is the density contrast between the fluid and the surrounding rock and η is the viscosity. Sakamaki et al. (2013) studied basaltic magmas and found that the fluid mobility $\Delta\rho/\eta$ of basalt melt ranges from 0.03 to 0.58 $g\times cm^{-3}\times Pa^{-1}\times s^{-1}$ at depths between 0 and 210 km. Kono et al. (2014) found that the $\Delta\rho/\eta$ of carbonate melt ranges from 101 to 148 $g\times cm^{-3}\times Pa^{-1}\times s^{-1}$ at depths between 30 and 180 km. It can be seen that the mobility of carbonate melt is hundreds to thousands of times higher than that of basaltic melts. However, Bajgain and Mookherjee (2021) found that the fluid mobility of aluminosilicate melts is several orders of magnitude lower than that of basalt melt. So, how does the presence of a large amount of water in aluminosilicate melts affect their fluid mobility? We calculated the $\Delta\rho/\eta$ of supercritical $NaAlSi_3O_8$–H_2O fluids using the density (3.537 g/cm^3) of olivine (Zha et al. 1998) as surrounding solid rock. In Fig. 6, the $\Delta\rho/\eta$ of supercritical $NaAlSi_3O_8$–H_2O fluids exhibit a linear relationship with pressure at various water contents. The $\Delta\rho/\eta$ of supercritical $NaAlSi_3O_8$–H_2O fluid with 30 wt% H_2O increases from

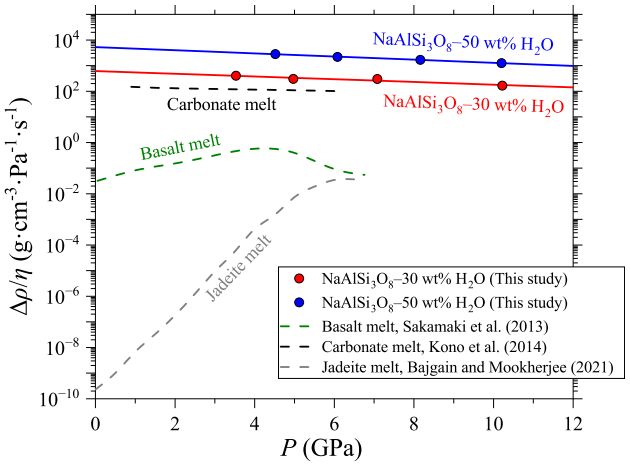

Fig. 6 The fluid mobility $\Delta\rho/\eta$ of supercritical $NaAlSi_3O_8$–H_2O fluid at 30 wt% H_2O and 50 wt% H_2O. The $\Delta\rho/\eta$ values for carbonate melt (Kono et al. 2014), basalt melt (Sakamaki et al. 2013), and Jadeite melt (Bajgain and Mookherjee 2021) are included for comparison

166 to 402 $g\times cm^{-3}\times Pa^{-1}\times s^{-1}$ as the pressure decreases from 10.2 to 3.5 GPa. For the supercritical $NaAlSi_3O_8$–H_2O fluid with 50 wt% H_2O, the $\Delta\rho/\eta$ increases from 1256 to 2833 as the pressure decreases from 10.2 to 4.5 GPa. The fluid mobility of supercritical $NaAlSi_3O_8$–H_2O fluids is several orders of magnitude higher than that of basalt melt and is also significantly greater than that of carbonate melt. In particular, a supercritical $NaAlSi_3O_8$–H_2O fluid with 50 wt% water content exhibits a mobility more than 10 times higher than that of carbonate melt. Our study indicates that supercritical fluids containing a high concentration of silicates still exhibit high mobility. As these supercritical fluids ascend from deeper regions to shallower depths, their mobility is further enhanced. This enhancement effect becomes more pronounced with increasing water content in the supercritical fluids. Even at low volume fractions, supercritical fluids can migrate from the subducting slab into the overlying mantle wedge, playing a significant role in the transport of elements.

6 Conclusion

In this study, we employed first-principles molecular dynamics simulations to investigate the $NaAlSi_3O_8$–H_2O systems with water contents of 30-wt% and 50-wt% at a temperature of 2000 K and under varying pressures. The results indicate that within the studied pressure range, properties such as structure, self-diffusion, and viscosity are closely related to pressure. In both systems, increasing pressure leads to a rise in the proportion of Q^2 species, with a corresponding decrease in Q^3 species in the 30-wt% H_2O system and a decrease in Q^0 species in the 50-wt% H_2O system. The average n of Q^n does not change in the system with 30% H_2O system, but shows a slight positive correlation with pressure in the system with 50 wt% H_2O system. The proportions of H_2O_m and Si–O–H in both systems decrease with increasing pressure, and the increasing water content can weaken the pressure effect on the proportions of H and O species. Within the studied pressure range, the self-diffusion coefficients of Na, O, and H decrease with increasing pressure. D_{Si} shows a weak positive correlation with pressure in the 30 wt% H_2O system, while it gradually decreases with increasing pressure in the 50 wt% H_2O system. Under the same pressure, D_{Al} is slightly larger than D_{Si}, and D_{Al} generally shows a slight increase with increasing pressure. The order of self-diffusion coefficients is $D_{Na} \approx D_H > D_O > D_{Al} \approx D_{Si}$. The viscosity of supercritical $NaAlSi_3O_8$–H_2O fluid shows a weak positive pressure dependence. By comparing the viscosities of anhydrous and hydrous silicate melts from previous studies, we found that the addition of water caused a transition from negative to positive pressure dependence of viscosity, corresponding to a structural change from polymerization to depolymerization. We also calculated the fluid mobility $\Delta\rho/\eta$ of supercritical $NaAlSi_3O_8$–H_2O fluid and found that their $\Delta\rho/\eta$ is several orders of magnitude higher than that of basalt melt and is also significantly greater than that of carbonate melt. As supercritical fluids rise from deeper regions to shallower depths, their fluid mobility increases further. This increase becomes more significant with higher water content in the supercritical fluids. Even at low volume fractions, these fluids can migrate from the subducting slab into the overlying mantle wedge, contributing significantly to element transport.

Acknowledgements This work was supported by the National Natural Science Foundation of China (No. 42373033) and the Fundamental Research Funds for the Central Universities (No. B240201111). We are grateful to the High-Performance Computing Platform of Hohai University for providing the computational resources.

Author contributions Ziteng Long: writing, investigation, visualization; Yicheng Sun: writing, investigation, methodology, review and editing, supervision.

Funding This article is funded by National Natural Science Foundation of China (42373033, Yicheng Sun), Fundamental Research Funds for the Central Universities (B240201111, Yicheng Sun).

Declarations

Conflicts of interest The authors declare no conflicts of interest.

References

Allen MP, Tildesley DJ, Banavar JR (1989) Computer simulation of liquids. Phys Today 42(3):105–106. https://doi.org/10.1063/1.2810937

Ardia P, Giordano D, Schmidt MW (2008) A model for the viscosity of rhyolite as a function of H_2O-content and pressure: a calibration based on centrifuge piston cylinder experiments. Geochim Cosmochim Acta 72(24):6103–6123. https://doi.org/10.1016/j.gca.2008.08.025

Ashley AW, Bajgain S, Mookherjee M (2024) Mobility of magmas within the Earth: insights from the elasticity and transport properties of hydrous albitic melts. Geochem Geophys Geosyst 25(6):e2024GC011510. https://doi.org/10.1029/2024gc011510

Audétat A, Keppler H (2004) Viscosity of fluids in subduction zones. Science 303(5657):513–516. https://doi.org/10.1126/science.1092282

Bajgain SK, Mookherjee M (2020) Structure and properties of albite melt at high pressures. ACS Earth Space Chem 4(1):1–13. https://doi.org/10.1021/acsearthspacechem.9b00187

Bajgain SK, Mookherjee M (2021) Carbon bearing aluminosilicate melt at high pressure. Geochim Cosmochim Acta 312:106–123. https://doi.org/10.1016/j.gca.2021.07.039

Bajgain SK, Peng Y, Mookherjee M, Jing ZC, Solomon M (2019) Properties of hydrous aluminosilicate melts at high pressures. ACS Earth Space Chem 3(3):390–402. https://doi.org/10.1021/acsearthspacechem.8b00157

Behrens H, Schulze F (2003) Pressure dependence of melt viscosity in the system $NaAlSi_3O_8$–$CaMgSi_2O_6$. Am Miner 88(8–9):1351–1363. https://doi.org/10.2138/am-2003-8-919

Dingwell DB (2006) Transport properties of magmas: diffusion and rheology. Elements 2(5):281–286. https://doi.org/10.2113/gselements.2.5.281

Fortier SM, Giletti BJ (1989) An empirical model for predicting diffusion coefficients in silicate minerals. Science 245(4925):1481–1484. https://doi.org/10.1126/science.245.4925.1481

Giordano D, Russell JK, Dingwell DB (2008) Viscosity of magmatic liquids: a model. Earth Planet Sci Lett 271(1–4):123–134. https://doi.org/10.1016/j.epsl.2008.03.038

Grimme S, Antony J, Ehrlich S, Krieg H (2010) A consistent and accurate *ab initio* parametrization of density functional dispersion correction (DFT-D) for the 94 elements H-Pu. J Chem Phys 132(15):154104. https://doi.org/10.1063/1.3382344

Hui HJ, Zhang YX, Xu ZJ, Del Gaudio P, Behrens H (2009) Pressure dependence of viscosity of rhyolitic melts. Geochim Cosmochim Acta 73(12):3680–3693. https://doi.org/10.1016/j.gca.2009.03.035

Hunt JD, Manning CE (2012) A thermodynamic model for the system SiO_2–H_2O near the upper critical end point based on quartz solubility experiments at 500–1100 °C and 5–20 kbar. Geochim Cosmochim Acta 86:196–213. https://doi.org/10.1016/j.gca.2012.03.006

Jin DS, Xiao YL, Tan DB, Wang YY, Wang XX, Li WC, Su W, Li XG (2023) Supercritical fluid in deep subduction zones as revealed by multiphase fluid inclusions in an ultrahigh-pressure metamorphic vein. Proc Natl Acad Sci USA 120(20):e2219083120. https://doi.org/10.1073/pnas.2219083120

Karki BB, Stixrude LP (2010a) Viscosity of $MgSiO_3$ liquid at Earth's mantle conditions: implications for an early magma ocean. Science 328(5979):740–742. https://doi.org/10.1126/science.1188327

Karki BB, Stixrude L (2010b) First-principles study of enhancement of transport properties of silica melt by water. Phys Rev Lett 104(21):215901. https://doi.org/10.1103/PhysRevLett.104.215901

Kennedy GC, Wasserburg GJ, Heard HC, Newton RC (1962) The upper three-phase region in the system SiO_2-H_2O. Am J Sci 260(7):501–521. https://doi.org/10.2475/ajs.260.7.501

Kessel R, Schmidt MW, Ulmer P, Pettke T (2005) Trace element signature of subduction-zone fluids, melts and supercritical liquids at 120–180 km depth. Nature 437(7059):724–727. https://doi.org/10.1038/nature03971

Kessel R, Pettke T, Fumagalli P (2015) Melting of metasomatized peridotite at 4–6 GPa and up to 1200 °C: an experimental approach. Contrib Miner Petrol 169(4):37. https://doi.org/10.1007/s00410-015-1132-9

Kono Y, Kenney-Benson C, Hummer D, Ohfuji H, Park C, Shen GY, Wang YB, Kavner A, Manning CE (2014) Ultralow viscosity of carbonate melts at high pressures. Nat Commun 5:5091. https://doi.org/10.1038/ncomms6091

Kresse G, Furthmüller J (1996a) Efficiency of ab-initio total energy calculations for metals and semiconductors using a plane-wave basis set. Comput Mater Sci 6(1):15–50. https://doi.org/10.1016/0927-0256(96)00008-0

Kresse G, Furthmüller J (1996b) Efficient iterative schemes for *ab initio* total-energy calculations using a plane-wave basis set. Phys Rev B Condens Matter 54(16):11169–11186. https://doi.org/10.1103/physrevb.54.11169

Kresse G, Hafner J (1993) Ab initio molecular dynamics for liquid metals. Phys Rev B Condens Matter 47(1):558–561. https://doi.org/10.1103/physrevb.47.558

Kresse G, Hafner J (1994) Ab initio molecular-dynamics simulation of the liquid-metal-amorphous-semiconductor transition in germanium. Phys Rev B Condens Matter 49(20):14251–14269. https://doi.org/10.1103/physrevb.49.14251

Kushiro I (1978) Viscosity and structural changes of albite ($NaAlSi_3O_8$) melt at high pressures. Earth Planet Sci Lett 41(1):87–90. https://doi.org/10.1016/0012-821X(78)90044-4

Lesher CE (2010) Self-diffusion in silicate melts: theory, observations and applications to magmatic systems. Rev Miner Geochem 72(1):269–309. https://doi.org/10.2138/rmg.2010.72.7

Liebske C, Behrens H, Holtz F, Lange RA (2003) The influence of pressure and composition on the viscosity of andesitic melts. Geochim Cosmochim Acta 67(3):473–485. https://doi.org/10.1016/S0016-7037(02)01139-0

Makhluf AR, Newton RC, Manning CE (2020) Experimental investigation of phase relations in the system $NaAlSi_3O_8$–H_2O at high temperatures and pressures: liquids relations, liquid–vapor mixing, and critical phenomena at deep crust–upper mantle conditions. Contrib Miner Petrol 175(8):76. https://doi.org/10.1007/s00410-020-01711-2

Manning C (2004) The chemistry of subduction-zone fluids. Earth Planet Sci Lett 223(1–2):1–16. https://doi.org/10.1016/j.epsl.2004.04.030

Manning CE, Frezzotti ML (2020) Subduction-zone fluids. Elements 16(6):395–400. https://doi.org/10.2138/gselements.16.6.395

McKenzie D (1989) Some remarks on the movement of small melt fractions in the mantle. Earth Planet Sci Lett 95(1–2):53–72. https://doi.org/10.1016/0012-821x(89)90167-2

Mibe K, Kanzaki M, Kawamoto T, Matsukage KN, Fei YW, Ono S (2007) Second critical endpoint in the peridotite-H_2O system. J Geophys Res 112(B3):2005JB004125. https://doi.org/10.1029/2005jb004125

Mibe K, Chou IM, Bassett WA (2008) In situ Raman spectroscopic investigation of the structure of subduction-zone fluids. J Geophys Res 113(B4):2007JB005179. https://doi.org/10.1029/2007jb005179

Mibe K, Kawamoto T, Matsukage KN, Fei YW, Ono S (2011) Slab melting versus slab dehydration in subduction-zone magmatism. Proc Natl Acad Sci USA 108(20):8177–8182. https://doi.org/10.1073/pnas.1010968108

Mori S, Ohtani E, Suzuki A (2000) Viscosity of the albite melt to 7 GPa at 2000 K. Earth Planet Sci Lett 175(1–2):87–92. https://doi.org/10.1016/s0012-821x(99)00284-8

Mysen B (2014) Water-melt interaction in hydrous magmatic systems at high temperature and pressure. Prog Earth Planet Sci 1(1):4. https://doi.org/10.1186/2197-4284-1-4

Newton RC, Manning CE (2002) Solubility of enstatite + forsterite in H_2O at deep crust/upper mantle conditions: 4 to 15 kbar and 700 to 900 °C. Geochim Cosmochim Acta 66(23):4165–4176. https://doi.org/10.1016/S0016-7037(02)00998-5

Newton RC, Manning CE (2008) Thermodynamics of SiO_2–H_2O fluid near the upper critical end point from quartz solubility measurements at 10 kbar. Earth Planet Sci Lett 274(1–2):241–249. https://doi.org/10.1016/j.epsl.2008.07.028

Ni H (2020) Properties and effects of supercritical geofluids. Bull Miner Petrol Geochem 39:443–447. https://doi.org/10.19658/j.issn.1007-2802.2020.39.036

Ni HW, Hui HJ, Steinle-Neumann G (2015) Transport properties of silicate melts. Rev Geophys 53(3):715–744. https://doi.org/10.1002/2015rg000485

Ni HW, Zhang L, Xiong XL, Mao Z, Wang JY (2017) Supercritical fluids at subduction zones: evidence, formation condition, and physicochemical properties. Earth Sci Rev 167:62–71. https://doi.org/10.1016/j.earscirev.2017.02.006

Ni HW, Xiao YL, Xiong XL, Liu XD, Gao CX, Chen YX, Li YG, Li WC, Guo X, Wang YY, Tan DB, Zhang L (2025) Formation and evolution of supercritical geofluid. Sci China Earth Sci 68(1):39–51. https://doi.org/10.1007/s11430-024-1453-5

Perdew JP, Burke K, Ernzerhof M (1996) Generalized gradient approximation made simple. Phys Rev Lett 77(18):3865–3868. https://doi.org/10.1103/PhysRevLett.77.3865

Reid JE, Poe BT, Rubie DC, Zotov N, Wiedenbeck M (2001) The self-diffusion of silicon and oxygen in diopside ($CaMgSi_2O_6$) liquid up to 15 GPa. Chem Geol 174(1–3):77–86. https://doi.org/10.1016/S0009-2541(00)00308-9

Reid JE, Suzuki A, Funakoshi KI, Terasaki H, Poe BT, Rubie DC, Ohtani E (2003) The viscosity of $CaMgSi_2O_6$ liquid at pressures up to 13 GPa. Phys Earth Planet Inter 139(1–2):45–54. https://doi.org/10.1016/S0031-9201(03)00143-2

Sakamaki T, Suzuki A, Ohtani E, Terasaki H, Urakawa S, Katayama Y, Funakoshi KI, Wang YB, Hernlund JW, Ballmer MD (2013) Ponded melt at the boundary between the lithosphere and asthenosphere. Nat Geosci 6:1041–1044. https://doi.org/10.1038/ngeo1982

Shen AH, Keppler H (1997) Direct observation of complete miscibility in the albite–H_2O system. Nature 385:710–712. https://doi.org/10.1038/385710a0

Stalder R, Ulmer P, Thompson AB, Günther D (2000) Experimental approach to constrain second critical end points in fluid/silicate systems: near-solidus fluids and melts in the system albite-H_2O. Am Miner 85(1):68–77. https://doi.org/10.2138/am-2000-0108

Sun YC, Liu XD, Lu XC (2023) Structures and transport properties of supercritical SiO_2-H_2O and $NaAlSi_3O_8$-H_2O fluids. Am Miner 108(10):1871–1880. https://doi.org/10.2138/am-2022-8724

Taniguchi H (1992) Entropy dependence of viscosity and the glass-transition temperature of melts in the system diopside-anorthite. Contrib Mineral Petrol 109(3):295–303. https://doi.org/10.1007/BF00283319

Thomas R, Davidson P (2016) Revisiting complete miscibility between silicate melts and hydrous fluids, and the extreme enrichment of some elements in the supercritical state: consequences for the formation of pegmatites and ore deposits. Ore Geol Rev 72:1088–1101. https://doi.org/10.1016/j.oregeorev.2015.10.004

Thomas R, Rericha A (2025) Extreme element enrichment by the interaction of supercritical fluids from the mantle with crustal rocks. Minerals 15(1):33. https://doi.org/10.3390/min15010033

Thomas R, Davidson P, Badanina E (2012) Water- and boron-rich melt inclusions in quartz from the malkhan pegmatite, transbaikalia, Russia. Minerals 2(4):435–458. https://doi.org/10.3390/min2040435

Tutolo BM, Luhmann AJ, Kong XZ, Saar MO, Seyfried WE (2015) CO_2 sequestration in feldspar-rich sandstone: coupled evolution of fluid chemistry, mineral reaction rates, and hydrogeochemical properties. Geochim Cosmochim Acta 160:132–154. https://doi.org/10.1016/j.gca.2015.04.002

Wang YB, Sakamaki T, Skinner LB, Jing ZC, Yu T, Kono Y, Park C, Shen GY, Rivers ML, Sutton SR (2014) Atomistic insight into viscosity and density of silicate melts under pressure. Nat Commun 5:3241. https://doi.org/10.1038/ncomms4241

Wang YY, Xiao YL, Chen RX, Chen YX, Li JL, Guo S (2025) Natural records of supercritical fluids in subduction zones. Earth Sci Rev 261:105031. https://doi.org/10.1016/j.earscirev.2024.105031

Zha CS, Duffy TS, Downs RT, Mao HK, Hemley RJ (1998) Brillouin scattering and X-ray diffraction of San Carlos olivine: direct pressure determination to 32 GPa. Earth Planet Sci Lett 159(1–2):25–33. https://doi.org/10.1016/S0012-821X(98)00063-6

Zheng YF, Xia QX, Chen RX, Gao XY (2011) Partial melting, fluid supercriticality and element mobility in ultrahigh-pressure metamorphic rocks during continental collision. Earth Sci Rev 107(3–4):342–374. https://doi.org/10.1016/j.earscirev.2011.04.004

Zheng YF, Chen RX, Xu Z, Zhang SB (2016) The transport of water in subduction zones. Sci China Earth Sci 59(4):651–682. https://doi.org/10.1007/s11430-015-5258-4